AMERICAN SOCIETY FOR MICROBIOLOGY | Journal of Bacteriology®

RESEARCH ARTICLE

Regulation of the *icl1* Gene Encoding the Major Isocitrate Lyase in *Mycobacterium smegmatis*

Eon-Min Ko,[a] Ju-Yeon Kim,[a] Sujin Lee,[b,c] Suhkmann Kim,[b,c] Jihwan Hwang,[a] Jeong-Il Oh[a]

[a]Department of Integrated Biological Science, Pusan National University, Busan, South Korea
[b]Department of Chemistry, Pusan National University, Busan, South Korea
[c]Chemistry Institute for Functional Materials, Pusan National University, Busan, South Korea

Eon-Min Ko and Ju-Yeon Kim contributed equally to this work. They are listed in alphabetical order by given name.

ABSTRACT *Mycobacterium smegmatis* has two isocitrate lyase (ICL) isozymes (MSMEG_0911 and MSMEG_3706). We demonstrated that ICL1 (MSMEG_0911) is the predominantly expressed ICL in *M. smegmatis* and plays a major role in growth on acetate or fatty acid as the sole carbon and energy source. Expression of the *icl1* gene in *M. smegmatis* was demonstrated to be strongly upregulated during growth on acetate relative to that in *M. smegmatis* grown on glucose. Expression of *icl1* was shown to be positively regulated by the RamB activator, and three RamB-binding sites (RamBS1, RamBS2, and RamBS3) were identified in the upstream region of *icl1* using DNase I footprinting analysis. Succinyl coenzyme A (succinyl-CoA) was shown to increase the affinity of binding of RamB to its binding sites and enable RamB to bind to RamBS2, which is the most important site for RamB-mediated induction of *icl1* expression. These results suggest that succinyl-CoA serves as a coinducer molecule for RamB. Our study also showed that cAMP receptor protein (Crp1; MSMEG_6189) represses *icl1* expression in *M. smegmatis* grown in the presence of glucose. Therefore, the strong induction of *icl1* expression during growth on acetate as the sole carbon source relative to the weak expression of *icl1* during growth on glucose is likely to result from combined effects of RamB-mediated induction of *icl1* in the presence of acetate and Crp-mediated repression of *icl1* in the presence of glucose.

IMPORTANCE Carbon flux through the glyoxylate shunt has been suggested to affect virulence, persistence, and antibiotic resistance of *Mycobacterium tuberculosis*. Therefore, it is important to understand the precise mechanism underlying the regulation of the *icl* gene encoding the key enzyme of the glyoxylate shunt. Using *Mycobacterium smegmatis*, this study revealed the regulation mechanism underlying induction of *icl1* expression in *M. smegmatis* when the glyoxylate shunt is required. The conservation of the *cis*- and *trans*-acting regulatory elements related to *icl1* regulation in both *M. smegmatis* and *M. tuberculosis* implies that a similar regulatory mechanism operates for the regulation of *icl1* expression in *M. tuberculosis*.

KEYWORDS acetate, cAMP, Crp, isocitrate lyase, glyoxylate shunt, *Mycobacterium*, regulation of gene expression, RamB, succinyl-CoA, tuberculosis

Citation Ko E-M, Kim J-Y, Lee S, Kim S, Hwang J, Oh J-I. 2021. Regulation of the *icl1* gene encoding the major isocitrate lyase in *Mycobacterium smegmatis*. J Bacteriol 203: e00402-21. https://doi.org/10.1128/JB.00402-21.

Editor Tina M. Henkin, Ohio State University

Address correspondence to Jeong-Il Oh, joh@pusan.ac.kr.

Received 3 August 2021
Accepted 9 September 2021
Accepted manuscript posted online 13 September 2021
Published 5 November 2021

Isocitrate lyase (ICL) catalyzes the cleavage of isocitrate to succinate and glyoxylate. The ICL-catalyzing reaction forms the glyoxylate shunt together with the reaction of malate synthase catalyzing the condensation of glyoxylate with acetyl coenzyme A (acetyl-CoA) to malate. The glyoxylate shunt forms a reaction cycle with reactions of the tricarboxylic acid (TCA) cycle, in which two molecules of acetyl-CoA yield one molecule of succinate as the net result. Therefore, the glyoxylate shunt is required for anaplerosis replenishing the reaction intermediates of the TCA cycle from acetyl-CoA when molecules such as acetate, fatty acids, or ketogenic amino acids are used as the sole carbon source (1). The glyoxylate shunt has been shown to play a crucial role in survival and persistence of *Mycobacterium tuberculosis* in both activated macrophages and mice (2, 3), implying that a metabolic shift in the principal carbon source from carbohydrates to fat might occur in *M. tuberculosis* residing within the host. Indeed, several lines of evidence have been reported which suggest that *M. tuberculosis* preferentially relies on fatty acids rather than carbohydrates when persisting inside the host (3–6). Based on the length and domain organization, ICLs are divided into three groups (3). The small prokaryotic ICLs belonging to group I consist of two domains (domains I and III), while the ICLs of group II, found in eukaryotes, have an additional domain (domain II) between the domains I and III. The mycobacterial ICLs of group III, which are similar to the group II ICLs and found in mycobacteria, are classified into an independent group due to the presence of the additional domain IV at their C termini. *M. tuberculosis* has two ICL isoforms. ICL1 is a prokaryotic type, while ICL2 is a mycobacterial ICL of group III (2, 3). The ICLs found in mycobacteria also possess the activity of methylcitrate lyase and thus function as key enzymes for the methylcitrate cycle that is involved in propionyl-CoA assimilation (5, 7–9). Since the isocitrate lyase and methylcitrate lyase activities of ICL2 were demonstrated to be substantially activated upon acetyl-CoA and propionyl-CoA binding, it was suggested that ICL2 might act as a gatekeeping enzyme to regulate the carbon flux between the TCA cycle and the glyoxylate shunt (10).

The genes (*icl1* or *aceA*) encoding ICL in *M. tuberculosis*, *Mycobacterium avium*, and *Mycobacterium smegmatis* have been shown to be upregulated when acetate or fatty acid is supplied as the sole carbon source (11–13). Interestingly, expression of the gene in *M. tuberculosis* has been shown to be also induced under hypoxic and low-pH conditions, as well as during infection of macrophages and mice (9, 14–17). Mycobacteria belong to the order *Corynebacteriales*, as does *Corynebacterium glutamicum*, which is a fast-growing environmental saprophyte (18). It was first demonstrated in *C. glutamicum* that RamB (regulator of acetate metabolism B) is involved in the negative regulation of the *aceA* gene encoding ICL (19, 20). Likewise, the RamB homolog of *M. tuberculosis* was also shown to act as a transcriptional repressor in the regulation of *icl1* (13). At the posttranscriptional level, the activity of ICL1 has been suggested to be controlled by acetylation and succinylation in *M. tuberculosis* (21–23).

Since carbon flux through the glyoxylate shunt has been suggested to affect virulence, persistence, and antibiotic resistance of *M. tuberculosis* (2, 3, 5, 24), it is important to understand the precise mechanism underlying the regulation of the *icl* gene encoding the key enzyme of the glyoxylate shunt. Although RamB has been demonstrated to be the master regulator functioning as a repressor in the regulation of *icl1* (*aceA*) expression in *M. tuberculosis* and *C. glutamicum*, there has been no report clearly revealing the nature of the effector molecule that modulates the functionality of RamB. Here, we demonstrate that succinyl-CoA serves as a coinducer for RamB and that RamB functions as a transcriptional activator for *icl1* expression in *M. smegmatis*, in contrast to the cases in *M. tuberculosis* and *C. glutamicum*. We also provide evidence that Crp1 (cAMP receptor protein; MSMEG_6189) is also implicated in the negative regulation of *icl1* expression in *M. smegmatis* during growth on glucose.

RESULTS

***M. smegmatis* has two ICLs, and ICL1 plays a major role in utilization of acetate and fatty acids.** *M. smegmatis* has two genes that encode ICL isozymes (*MSMEG_0911* and *MSMEG_3706*). The *MSMEG_0911* (*icl1*) gene encodes a protein composed of 428 amino acids, which is closely related to the prokaryotic ICLs of group I, while the predicted *MSMEG_3706* (*icl2*) gene product, consisting of 769 amino acids, is closely homologous to the mycobacterial ICLs belonging to group III. ICL1 and ICL2 of *M. smegmatis* show 92% and 77% sequence identity to ICL1 (MT0483) and ICL2 (MT1966) of *M. tuberculosis* CDC1551, respectively.

To evaluate the functional roles of the *icl1* and *icl2* genes in utilization of acetate and fatty acids in *M. smegmatis*, null mutants of *M. smegmatis* carrying deletions within *icl1*, *icl2*, or both *icl1* and *icl2* were constructed, and the wild-type (WT) and mutant

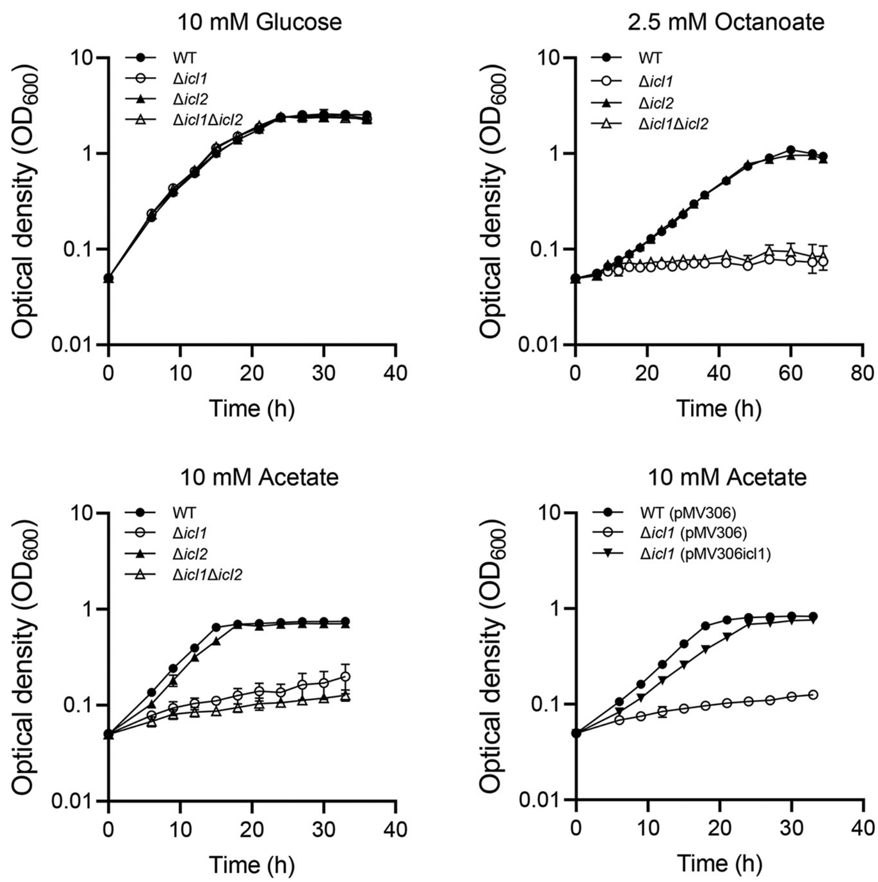

FIG 1 Growth of the WT, Δ*icl1*, Δ*icl2*, and Δ*icl1* Δ*icl2* strains of *M. smegmatis* on various carbon sources. The Δ*icl1*, Δ*icl2*, and Δ*icl1* Δ*icl2* mutant strains, as well as the WT strain as a control, were grown aerobically at 37°C in 7H9 medium supplemented with 10 mM glucose, 10 mM acetate, or 2.5 mM octanoate as the sole carbon source. For complementation of the Δ*icl1* mutant, pMV306icl1 (a pMV306-derived plasmid carrying the intact *icl1* gene and its own promoter) was introduced into the Δ*icl1*mutant. The Δ*icl1* strain harboring pMV306icl1, as well as the WT and Δ*icl1* strains with the empty vector pMV306, was grown aerobically in 7H9-acetate at 37°C. All values provided were determined from three biological replicates. The error bars indicate the standard deviations.

strains were examined for their growth in medium supplemented with glucose, acetate, or octanoate as the sole carbon source (Fig. 1). No difference between the WT and mutant strains was observed with regard to growth rate when glucose was supplied as a carbon source. When acetate was supplied as the sole carbon source, the Δ*icl1* mutant strain showed significantly impaired growth, with a doubling time of 21.4 h, compared to the WT strain, showing a doubling time of 4.2 h. In contrast, growth of *M. smegmatis* on acetate was marginally affected by *icl2* mutation. Cumulative effects of the *icl1* and *icl2* mutations on growth on acetate were observed for the Δ*icl1* Δ*icl2* mutant strain. Introduction of the pMV306icl1 plasmid carrying the intact *icl1* gene into the Δ*icl1* mutant restored growth of the mutant on acetate, indicating that the severe defect in acetate utilization observed for the Δ*icl1* mutant was the result of *icl1* inactivation. When octanoate was supplied as the sole carbon source, the WT and Δ*icl2* mutant strains showed the same growth rate. In contrast, the Δ*icl1* and Δ*icl1* Δ*icl2* mutant strains did not grow under the same condition, indicating that ICL1 is indispensable for growth of *M. smegmatis* on octanoate. Taken together, the results presented in Fig. 1 suggest that ICL1 serves as the major ICL in *M. smegmatis* during growth on acetate and fatty acids. The relative expression levels of *icl1* and *icl2* could be extrapolated from the reads per kilobase pair per million (RPKM) of *icl1* and *icl2* obtained from RNA sequencing analysis on *M. smegmatis* grown aerobically on glucose (25). The RPKM

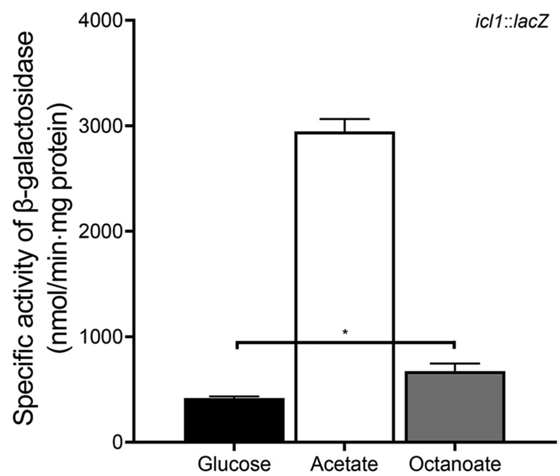

FIG 2 Expression levels of the *icl1* gene in *M. smegmatis* grown on glucose, acetate, or octanoate. The WT strain of *M. smegmatis* strain containing the *icl1*::*lacZ* translational fusion plasmid pNCIIicl1 was grown aerobically to an OD_{600} of 0.45 to 0.5 in 7H9 medium supplemented with 10 mM glucose, 10 mM acetate, or 2.5 mM octanoate as the sole carbon source. Cell-free crude extracts were used to measure β-galactosidase activity. All values provided were determined from three biological replicates. The error bars indicate the standard deviations. *, $P < 0.01$.

value of *icl1* was found to be 43-fold greater than that of *icl2*, indicating that ICL1 is the predominantly expressed ICL in *M. smegmatis* (the RPKM values of *icl1* and *icl2* are 895.5 and 20.7, respectively).

Expression of *icl1* is induced in the presence of acetate and fatty acids. Acetate and fatty acids are metabolized to acetyl-CoA through acetate activation and β-oxidation, respectively (11). When *M. smegmatis* utilizes acetate or fatty acid as the sole carbon source, the glyoxylate shunt is required to replenish TCA cycle intermediates from acetyl-CoA. We assessed whether expression of *icl1* is induced in *M. smegmatis* grown on acetate or fatty acids. The expression level of the *icl1* gene in *M. smegmatis* grown on glucose, acetate, or octanoate was examined using the WT strain carrying the *icl1*::*lacZ* translational fusion plasmid pNCIIicl1. As shown in Fig. 2, expression of *icl1* was induced 7-fold in *M. smegmatis* grown on acetate relative to that in *M. smegmatis* grown on glucose, while only a 1.6-fold increase in *icl1* expression was observed in *M. smegmatis* grown on octanoate relative to *M. smegmatis* grown on glucose. We also determined *icl2* expression using the WT strain carrying the *icl2*::*lacZ* translational fusion plasmid pNCIIicl2. The *icl2* gene was expressed only marginally irrespective of whether glucose or acetate was supplied as the sole carbon source (data not shown).

RamB serves as a transcriptional activator for *icl1* expression. To understand the regulation mechanism underlying induction of *icl1* expression by acetate in *M. smegmatis*, we first searched for the gene homologous to the *ramB* gene, whose product had been found to regulate expression of several genes related to acetate metabolism in *C. glutamicum* and *M. tuberculosis* (13, 19). A BLAST analysis revealed that the chromosome of *M. smegmatis* contains a gene (*MSMEG_0906*) the product of which shows 86% and 55% sequence identity to RamB (Rv0465c and Cg0444) of *M. tuberculosis* and *C. glutamicum*, respectively. The *ramB* gene is located in the vicinity of the *icl1* gene on the chromosomes of both *M. smegmatis* and *M. tuberculosis* (Fig. 3).

To gain insight into the functional role of the *ramB* gene in utilization of acetate in *M. smegmatis*, a Δ*ramB* mutant of *M. smegmatis* was constructed, and the mutant was compared with the WT strain for growth in medium supplemented with glucose or acetate (see Fig. S1 in the supplemental material). No difference between the WT and Δ*ramB* mutant strains was observed with respect to growth rate when glucose was supplied as the sole carbon source (the doubling times of the WT and mutant strains were 4.8 h). When acetate was the sole carbon source, growth of the Δ*ramB* mutant strain was retarded compared to that of the WT strain (the doubling times of the WT

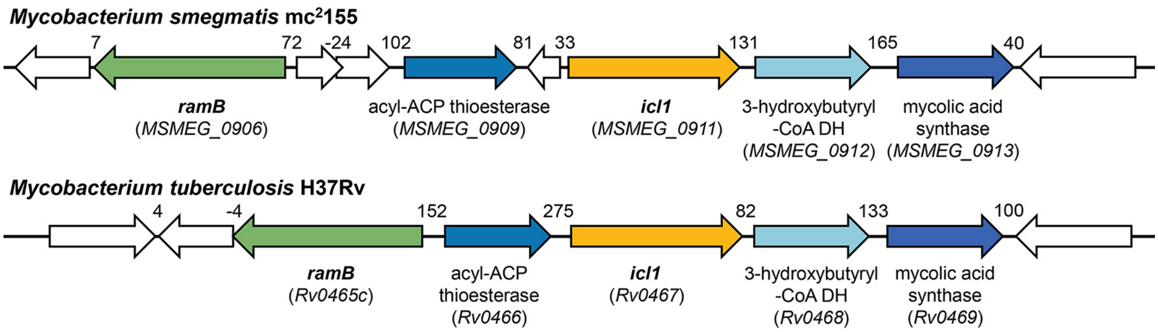

FIG 3 Genetic organizations of the loci associated with the *icl1* and *ramB* genes in *M. smegmatis* and *M. tuberculosis*. The open reading frames are shown as arrows, whose size and orientation indicate their relative length and direction, respectively. The lengths of the overlapping and intergenic regions are given as negative and positive nucleotide numbers above the schematic diagrams, respectively.

and mutant strains were 4.8 h and 6.8 h, respectively), indicating that RamB is necessary for the optimal growth of *M. smegmatis* on acetate. To determine the functional role of RamB in the regulation of *icl1* expression in *M. smegmatis*, expression of the *icl1* gene was examined in the WT and Δ*ramB* mutant strains of *M. smegmatis* carrying pNCIIicl1 (Fig. 4). Consistent with the result in Fig. 2, the expression level of *icl1* was shown to be increased 6.5-fold in the WT strain grown on acetate relative to that in the WT strain grown on glucose. The *icl1* gene was significantly less expressed in the Δ*ramB* mutant grown on acetate than in the WT strain grown under the same condition, and the lower expression level of *icl1* in the mutant relative to the WT strain was also observed when glucose was supplied as the sole carbon source. These results indicate that RamB serves as a transcriptional activator for the *icl1* gene in *M. smegmatis*. Introduction of the intact *ramB* gene into the Δ*ramB* mutant led to restoration of the expression level of *icl1* to that observed in the WT strain when the strains were grown on acetate. We also found that RamB of *M. smegmatis* negatively regulated its own gene irrespective of whether it was grown on glucose or acetate (Fig. S2).

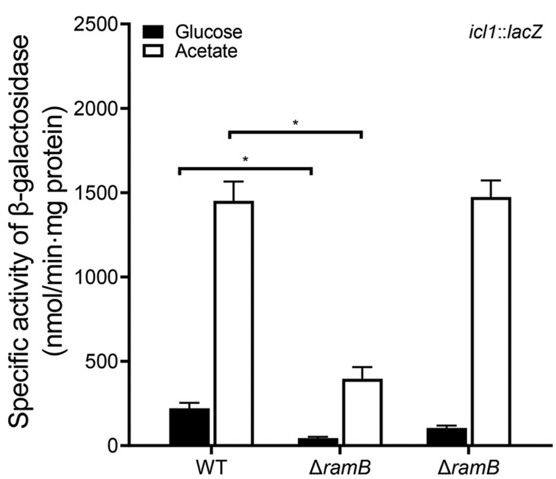

FIG 4 Expression levels of the *icl1* gene in the WT and Δ*ramB* mutant strains of *M. smegmatis*. The WT and Δ*ramB* mutant strains carrying both the empty vector pMV306 and the *icl1*::*lacZ* translational fusion plasmid pNCIIicl1 were used in the experiment. For complementation of the Δ*ramB* mutant, pMV306ramB (a pMV306-derived plasmid carrying the intact *ramB* gene and its own promoter) was introduced into the mutant in place of pMV306. The strains were grown aerobically to an OD_{600} of 0.45 to 0.5 in 7H9 medium supplemented with 10 mM glucose or 10 mM acetate as the carbon source. Cell-free crude extracts were used to measure *β*-galactosidase activity. All values provided were determined from three biological replicates. The error bars indicate the standard deviations. *, $P < 0.01$.

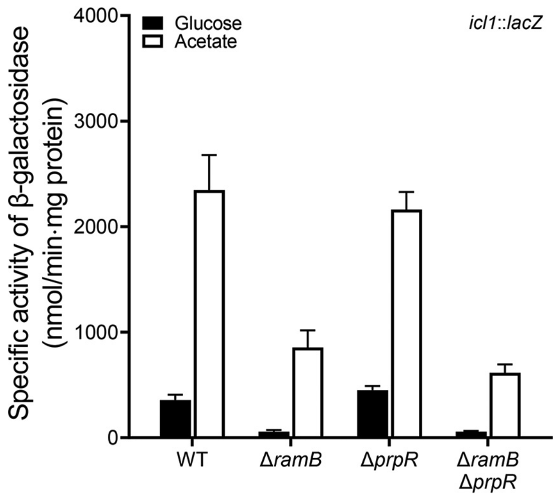

FIG 5 Expression levels of the *icl1* gene in the WT, Δ*ramB*, Δ*prpR*, and Δ*ramB* Δ*prpR* mutant strains of *M. smegmatis*. The WT, Δ*ramB*, Δ*prpR*, and Δ*ramB* Δ*prpR* mutant strains containing the *icl1*::*lacZ* translational fusion plasmid pNCIIicl1 were grown aerobically to an OD_{600} of 0.45 to 0.5 in 7H9 medium supplemented with 10 mM glucose or 10 mM acetate as the sole carbon source. Cell-free crude extracts were used to measure β-galactosidase activity. All values provided were determined from three biological replicates. The error bars indicate the standard deviations.

It was previously demonstrated that PrpR (propionate regulator), a homolog of RamB, positively regulated the *icl1* gene in *M. tuberculosis* and *M. smegmatis* when they were grown on propionate (26). PrpR (MSMEG_6643) of *M. smegmatis* shows 48% sequence identity and 65% similarity to RamB (MSMEG_0906), and the amino acid sequences of their DNA binding helix-turn-helix domains are similar to each other. Since the PrpR-binding sequence was demonstrated to be similar to the RamB-binding sequence (26), it is possible that PrpR is involved in induction of *icl1* expression in *M. smegmatis* during growth on acetate. To verify this assumption, null mutants of *M. smegmatis* carrying deletions within *prpR* or both *ramB* and *prpR* were constructed, and the expression level of the *icl1* gene was determined using the WT, Δ*ramB*, Δ*prpR*, and Δ*ramB* Δ*prpR* strains of *M. smegmatis* carrying pNCIIicl1. As shown in Fig. 5, inactivation of the *prpR* gene in the background of the WT and Δ*ramB* mutant strains resulted in only a marginal decrease in *icl1* expression when the strains were grown on acetate. In conjunction with the previous report (26), this result indicates that PrpR plays a specific role in *icl1* induction by propionate but not by acetate.

Identification of the RamB-binding sites in the upstream region of *icl1*. Despite the importance of RamB in the regulation of *aceA* (*icl1*), the nature of its effector molecule has remained elusive. Based on structural and mutational studies on PrpR, Tang et al. have recently predicted that succinyl-CoA might be an effector molecule that can bind to RamB (27). To define precisely the number and location of RamB-binding sites in the *icl1* upstream region as well as the effect of succinyl-CoA on binding of RamB to the DNA region, DNase I footprinting analysis was conducted with purified RamB and 6-carboxytetramethylrhodamine (TAMRA)-labeled DNA fragments containing the *icl1* upstream region in the presence or absence of succinyl-CoA (Fig. 6). In the absence of succinyl-CoA in the reaction mixtures, binding of RamB protected the 24-bp DNA region from DNase I cleavage at positions -96 to -73 (RamBS1) with respect to the transcriptional start point (TSP). The addition of 200 μM succinyl-CoA to the reaction mixtures resulted in a more clearly protected window for RamBS1 and protection of two additional DNA regions at positions -65 to -42 (RamBS2) and -5 to $+19$ (RamBS3). The binding affinity of RamB for the binding sites appeared to be in descending order of RamBS1, RamBS2, and RamBS3. The sequence of RamBS1 (T<u>T</u>C<u>T</u>TCA<u>CAA</u>TC<u>TT</u>C<u>GCAA</u>GTT<u>AA</u>; the conserved nucleotides in both RamBS1 and RamBS2 are underlined) is similar to that of RamBS2 (G<u>T</u>T<u>T</u>CGC<u>CAA</u>AA<u>TT</u>G<u>GCAA</u>AGG<u>AA</u>),

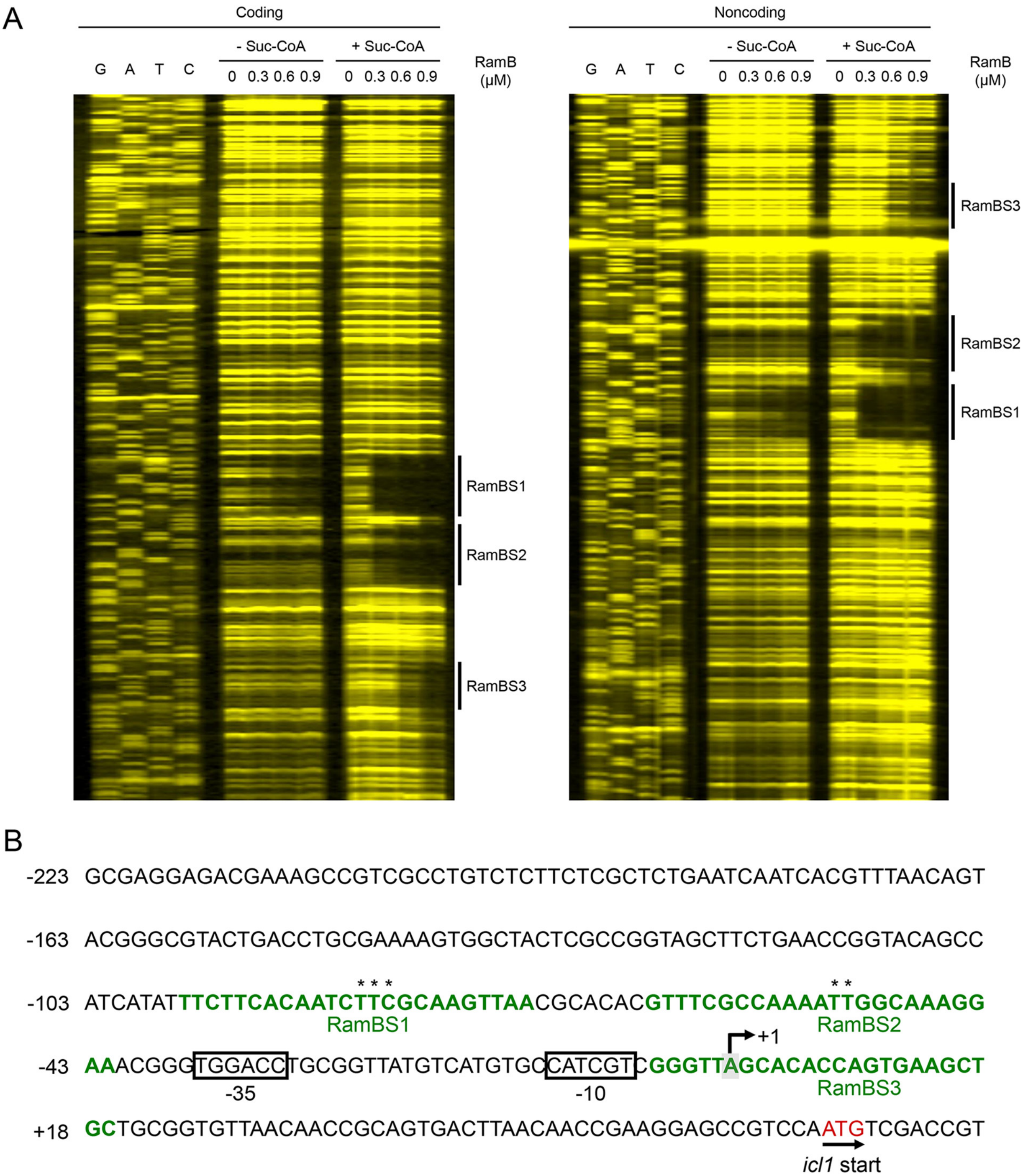

FIG 6 Binding of RamB to the *icl1* regulatory region. (A) DNase I footprinting analysis of the *icl1* regulatory region bound by purified RamB. The DNA fragments containing the coding and noncoding strands labeled with TAMRA at their 5′ ends were incubated with increasing concentrations of purified RamB (0.3, 0.6, and 0.9 μM) in the absence (- Suc-CoA) or presence (+ Suc-CoA) of 200 μM succinyl-CoA and then subjected to DNase I footprinting reactions. The amounts of RamB protein used are given above the lanes. The regions protected by RamB, which indicate the RamB-binding sites, are marked by thick black lines (RamBS1, RamBS2, and RamBS3). Lanes G, A, T, and C represent the sequence ladders. (B) The upstream sequence of the *icl1* gene, including its putative promoter region and the identified *cis*-acting regulatory elements involved in the regulation of the *icl1* gene. The RamB-binding sites (RamBS1, RamBS2, and RamBS3) are indicated in green font. The nucleotides in RamBS1 and RamBS2 which were mutated for the promoter assay in Fig. 7 are indicated with asterisks. The TSP of the *icl1* gene is marked by +1. The putative promoter region (−35 and −10) of the *icl1* gene is boxed. The start codon of *icl1* is indicated both in red font and by the arrow indicating the transcriptional direction. The numbers on the left side of the sequences show the positions of the leftmost nucleotides relative to the TPS of the *icl1* gene.

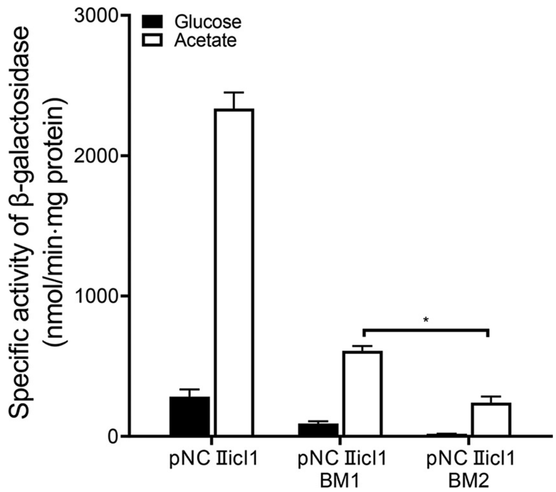

FIG 7 Effects of mutations in the RamB-binding sites (RamBS1 and RamBS2) on *icl1* expression. The *icl1* promoter activities were determined by using the pNCIIicl1-derived translational fusion plasmids (pNCIIicl1BM1 and pNCIIicl1BM2) with mutations in RamBS1 and RamBS2, respectively. As a control, pNCIIicl1 was included in the experiment. The WT strain of *M. smegmatis* harboring the translational fusion plasmids was grown aerobically to an OD_{600} of 0.45 to 0.5 in 7H9 medium supplemented with 10 mM glucose or 10 mM acetate as the sole carbon source. Cell-free crude extracts were used to measure β-galactosidase activity. All values provided were determined from three biological replicates. The error bars indicate the standard deviations. *, $P < 0.01$.

while the sequence of RamBS3 (GGGTTAGCACACCAGTGAAGCTGC) deviates from those of RamBS1 and RamBS2, which explains the low binding affinity of RamB for RamBS3. We also examined whether succinate, acetate, and acetyl phosphate (an intermediate of acetate activation) alter the binding affinity of RamB for the *icl1* regulatory region using electrophoretic mobility shift assay (EMSA). We did not perform EMSA with acetyl-CoA, because it had been reported that acetyl-CoA did not change the binding affinity of RamB for its binding site (19). As shown in Fig. S3, the presence of succinate, acetate, or acetyl phosphate in the EMSA reaction mixtures did not lead to noticeable changes in binding of RamB to the *icl1* regulatory region, in contrast to the presence of succinyl-CoA. Taken together, the DNase I footprinting and EMSA results clearly suggest that succinyl-CoA leads to changes in both binding affinity and binding patterns of RamB for the *icl1* regulatory region.

In order to ascertain the roles of the major RamB-binding sites (RamBS1 and RamBS2) in the regulation of *icl1* expression in *M. smegmatis*, we determined the effect of RamBS1 and RamBS2 mutations on *icl1* expression in the WT strain of *M. smegmatis* grown on glucose or acetate by using pNCIIicl1 derivatives that contain mutations within either RamBS1 or RamBS2 (Fig. 7). Transversion mutations were introduced into RamBS1 (CAATC<u>TTC</u>GCAAG to CAATC<u>GAG</u>GCAAG) and RamBS2 (CAAAA<u>TT</u>GGCAAA to CAAAA<u>GA</u>GGCAAA) on pNCIIicl1 to construct pNCIIicl1BM1 and pNCIIicl1BM2, respectively (the mutated nucleotides are underlined). As expected, expression of *icl1* was strongly induced by acetate in the control WT strain with pNCIIicl1. Expression of *icl1* from pNCIIicl1BM2 was significantly reduced compared to that from pNCIIicl1 when the *M. smegmatis* strains were grown on acetate. Mutations in RamBS1 affected *icl1* expression to a lesser extent than those in RamBS2, indicating that RamBS2 is more important in activation of *icl1* transcription than RamBS1.

By means of ^{1}H nuclear magnetic resonance (NMR) analysis, we tried to determine the level of succinyl-CoA in the WT strain of *M. smegmatis* grown on glucose or acetate to see whether the level of succinyl-CoA correlates with the expression level of *icl1*. We failed to detect succinyl-CoA using this analytical method. However, a 2-fold increase in succinate levels was observed in *M. smegmatis* grown on acetate relative to *M. smegmatis* grown on glucose (Fig. S4). This finding might indirectly imply an increased

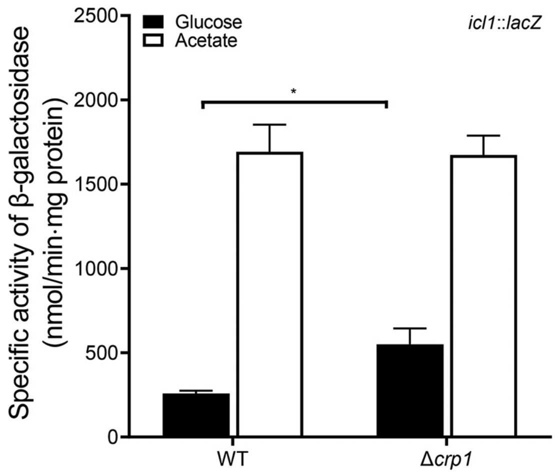

FIG 8 Expression levels of the *icl1* gene in the WT and Δ*crp1* mutant strains of *M. smegmatis*. The WT and Δ*crp1* mutant strains containing the *icl1::lacZ* translational fusion plasmid pEMIIicl1 were grown aerobically to an OD_{600} of 0.45 to 0.5 in 7H9 medium supplemented with 10 mM glucose or 10 mM acetate as the sole carbon source. Cell-free crude extracts were used to measure β-galactosidase activity. All values provided were determined from three biological replicates. The error bars indicate the standard deviations. *, $P < 0.01$.

cellular level of succinyl-CoA in *M. smegmatis* grown on acetate, given that succinyl-CoA is the preceding intermediate of succinate in the TCA cycle.

Crp is involved in repression of *icl1* in the presence of glucose. The Δ*ramB* Δ*prpR* mutant of *M. smegmatis* still showed the residual acetate-inducible regulation of *icl1* (Fig. 5), which implies that a regulatory system(s) other than RamB and PrpR still operates to increase *icl1* expression in *M. smegmatis* during growth on acetate (Fig. 5). The genome of *M. smegmatis* has two genes (*crp1* [*MSMEG_6189*] and *crp2* [*MSMEG_0539*]) encoding the cAMP receptor protein (Crp) paralogs that show 78% sequence identity to each other at the amino acid level (28, 29). Crp1 was demonstrated to be the major Crp that is predominantly expressed in *M. smegmatis* (30). Interestingly, it was observed in our previous RNA sequencing analysis that the Δ*crp1* mutant of *M. smegmatis* exhibited higher expression of *icl1* than the isogenic WT strain when both strains were grown on glucose (30). Consistent with the RNA sequencing result, expression of *icl1* was shown to be derepressed in the Δ*crp1* mutant grown on glucose relative to that in the WT strain grown on glucose, and this derepression was not observed during growth on acetate (Fig. 8). This result indicates that *icl1* is under the negative regulation of Crp1 in *M. smegmatis* during growth on glucose. Since Crp is a regulatory protein that controls gene expression in response to changes in cAMP levels, we determined whether the intracellular level of cAMP in *M. smegmatis* is changed depending on the carbon source in growth medium. As shown in Fig. 9, the cellular levels of cAMP in the WT strain of *M. smegmatis* grown on glucose and octanoate were found to be 1.7- and 1.8-fold higher than that in the same strain grown on acetate, respectively, which suggests that increased levels of cAMP might lead to Crp-mediated repression of *icl1* expression in *M. smegmatis* during growth on glucose or octanoate.

DISCUSSION

In this study, we demonstrated that ICL1 functions as the major ICL in the glyoxylate shunt that is required for growth of *M. smegmatis* on acetate or fatty acid as the sole carbon source, which is probably due to the very marginal expression of *icl2* relative to *icl1*. In contrast to the constitutive expression of *icl2*, expression of *icl1* was shown to be strongly (~7-fold) induced in *M. smegmatis* when acetate was used as the sole carbon source. This result is consistent with the previous report that 8-fold-higher ICL activity was detected in *M. smegmatis* grown on acetate than in *M. smegmatis*

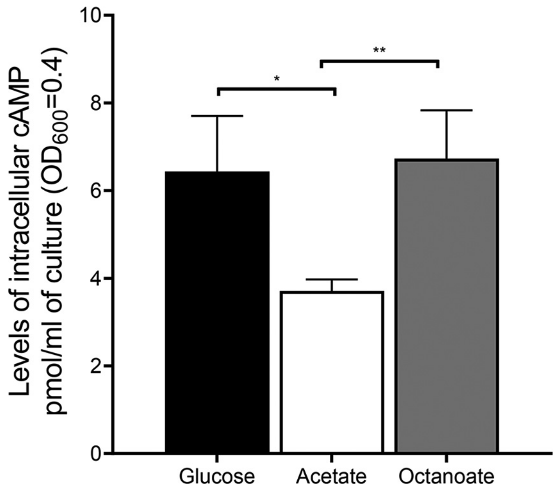

FIG 9 Effects of the carbon source on intracellular levels of cAMP in *M. smegmatis*. The WT strain of *M. smegmatis* was grown aerobically to an OD_{600} of 0.45 to 0.5 in 7H9 medium supplemented with 10 mM glucose, 10 mM acetate, or 2.5 mM octanoate as the sole carbon source. cAMP quantification was performed as described in Materials and Methods. All values provided are the average of the results from three biological replicates. The error bars indicate the standard deviations. *, $P < 0.05$; **, $P < 0.01$.

grown on glucose (31). In *C. glutamicum* and *M. tuberculosis*, the *aceA* and *icl1* genes are also upregulated during growth on acetate, which is achieved by RamB-mediated negative regulation in the absence of acetate (13, 19). In contrast to the RamB repressor in *M. tuberculosis*, the RamB homolog of *M. smegmatis* serves as an activator for *icl1* expression in the presence and absence of acetate despite a high (86%) sequence identity between the RamB proteins of *M. smegmatis* and *M. tuberculosis*. Using DNase I footprinting analysis, we identified three RamB-binding sites (RamBS1, RamBS2, and RamB3), two (RamBS1 and RamBS2) of which contain the sequences similar to the known RamB-binding motif (AA/GAACTTTGCAAA) (19). In the absence of succinyl-CoA, RamB was shown to preferentially bind to RamBS1, indicating that RamBS1 is the high-affinity binding site for RamB. Importantly, the presence of succinyl-CoA was shown to cause the binding of RamB to two additional sites, RamBS2 and RamBS3, as well as an increase in the binding affinity of RamB for RamBS1. The binding affinity of RamB for RamBS3 is noticeably weaker than that for RamBS1 and RamBS2 in the presence of succinyl-CoA, and RamBS3 overlaps the TSP of *icl1*. Therefore, it is unlikely that RamBS3 is involved in the positive regulation of *icl1*. We found that mutations in RamBS2 resulted in a more severe defect in *icl1* expression than those in RamBS1. The RamBS2 site was found to be located at positions −65 to −42 relative to the TSP of *icl1*, which is in line with the widely accepted principle that transcriptional activators generally bind upstream of their target promoters between positions −30 and −80 to enhance the binding of RNA polymerase to the promoters or the formation of an open complex (32, 33). Given both the location of RamBS2 and the result of site-directed mutagenesis on RamBS1 and RamBS2 (Fig. 7), it can be assumed that binding of RamB to RamBS2 might be directly involved in transcriptional activation of *icl1* and that RamB bound at the high-affinity binding site RamBS1 might facilitate binding of RamB to RamBS2. Given that the centers of RamBS1 and RamBS2 are separated by three helical turns (31 bp), two RamB proteins are expected to bind to RamBS1 and RamBS2 on the same phase of DNA, which probably enables the cooperative binding of RamB to RamBS1 and RamBS2. Taken together, the results of DNase I footprinting and mutagenesis analyses indicate that succinyl-CoA serves as a coinducer for the RamB activator in the regulation of *icl1* expression. It is especially noteworthy that the positions of three RamB-binding sites relative to the TSP as well as the *icl1* promoter sequences are also well conserved upstream of *icl1* in *M. tuberculosis* (see Fig. S5 in the supplemental material). We cannot explain why expression of *icl1* is not positively but negatively regulated by RamB in *M. tuberculosis* despite the conservation of the *cis*-acting regulatory elements for *icl1* in *M. smegmatis* and *M. tuberculosis*. To explain this disparity, a reassessment of the regulation of *icl1* expression in *M. tuberculosis* appears to be necessary.

The cellular level of succinyl-CoA is determined by a balance between its synthesis and consumption for biosynthesis of cellular constituents. Succinyl-CoA can be produced from α-ketoglutarate (αKG) and succinate in the TCA cycle, as well as from methylmalonyl-CoA by methylmalonyl-CoA mutase in propionyl-CoA metabolism (34, 35). The oxidation of αKG to succinate in the TCA cycle of *M. smegmatis* and *M. tuberculosis* has been suggested to occur in two separate metabolic routes. αKG is oxidized to succinate via succinyl-CoA through two sequential reactions catalyzed by αKG:ferredoxin (Fd) oxidoreductase and succinyl-CoA synthetase (35). The conventional αKG dehydrogenase complex composed of E1o, E2 (DlaT or SucB), and E3 (Lpd) has been suggested to play, at most, a minor role in the oxidation of αKG in the TCA cycle of *M. smegmatis* and *M. tuberculosis* (36, 37). As an alternative route for the oxidation of αKG to succinate, E1o alone without association with E2 and E3 catalyzes decarboxylation of αKG to succinic semialdehyde (SSA), which is subsequently oxidized to succinate by SSA dehydrogenase (37). In the presence of glyoxylate, the E1o protein was demonstrated to function mainly as a carboligase that catalyzes the ligation of αKG and glyoxylate with the concomitant release of CO_2 to yield 2-hydroxy-3-oxoadipate (HOA) (38), indicating that E1o serves as an HOA synthase or αKG decarboxylase, depending on the presence or absence of glyoxylate. Furthermore, it was suggested that αKG decarboxylase is predominantly utilized in oxidation of αKG to succinate in the TCA cycle when *M. smegmatis* is grown on glucose or glycerol, while αKG:Fd oxidoreductase was suggested to be important for mycobacterial growth under conditions that requires the glyoxylate shunt at ambient CO_2 levels (35, 39). Additionally, the GAS (glyoxylate shunt, anaplerotic fixation of CO_2, and succinyl-CoA synthetase for the generation of succinyl-CoA) pathway was suggested to operate in mycobacteria, which connects the glyoxylate shunt with the generation of succinyl-CoA (40). Carbon flux through the glyoxylate shunt was shown to be negligible in *M. smegmatis* grown on glucose (31), which is in line with our observation that the WT and Δ*icl1* Δ*icl2* mutant strains of *M. smegmatis* showed the same growth rate when they were grown on glucose (Fig. 1). The cellular levels of glyoxylate and succinate were demonstrated to rise in *M. smegmatis* when *icl1* expression was increased (Fig. S4) (41). Taken together, the above-described findings allow us to present a model for RamB-dependent induction of *icl1* expression in *M. smegmatis* grown on acetate (Fig. 10). When *M. smegmatis* is grown on acetate, the glyoxylate shunt is required for anaplerosis of the TCA cycle intermediates. As a result of increased carbon flux through the glyoxylate shunt, the cellular level of glyoxylate rises, which is expected to make E1o preferentially function as an HOA synthase rather than as an αKG decarboxylase. Due to the diminished αKG decarboxylase activity and inhibition of SSA dehydrogenase by glyoxylate (42), the oxidation of αKG is likely to proceed mainly by the succinyl-CoA-generating αKG:Fd oxidoreductase in the TCA cycle. On the other hand, the glyoxylate shunt is not necessary for growth of *M. smegmatis* on glucose, and thus, carbon flux through the glyoxylate shunt is minimal. The marginal cellular level of glyoxylate allows E1o to serve as an αKG decarboxylase that converts αKG to SSA. As suggested previously (35), αKG decarboxylase, which does not produce succinyl-CoA, is predominantly utilized in oxidation of αKG to succinate in the TCA cycle under these conditions. Therefore, the cellular level of succinyl-CoA is assumed to be lower in *M. smegmatis* during growth on glucose than in *M. smegmatis* grown on acetate wherein αKG:Fd oxidoreductase and the GAS pathway produce succinyl-CoA. The increased cellular level of succinyl-CoA in *M. smegmatis* during growth on acetate enables RamB-mediated induction of *icl1* expression.

Expression of *icl1* in *M. tuberculosis* has been demonstrated to be induced under respiration-inhibitory conditions such as hypoxic and low-pH conditions (9, 15–17).

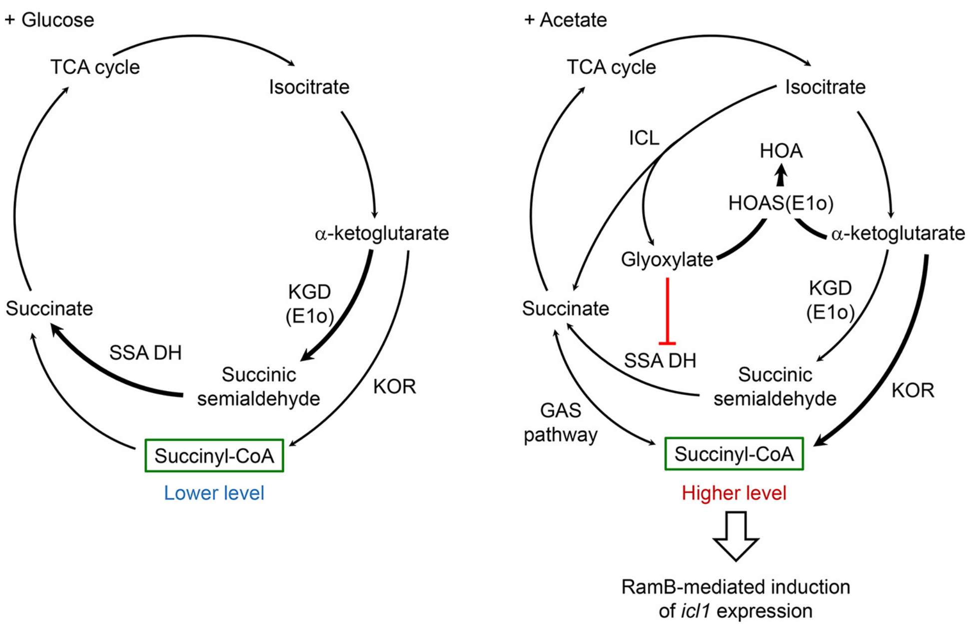

FIG 10 Model for RamB-mediated induction of *icl1* expression in *M. smegmatis* during growth on acetate. The simplified TCA cycle and glyoxylate shunt in *M. smegmatis* grown on glucose (+ Glucose) or acetate (+ Acetate) are depicted. When two or more alternative pathways are possible, the major pathways are indicated by thick arrows. Succinyl-CoA, which was used as a coinducer of RamB, is highlighted by green boxes. Abbreviations: HOA, 2-hydroxy-3-oxoadipate; HOAS, HOA synthase; ICL, isocitrate lyase; KOR, α-ketoglutarate: ferredoxin oxidoreductase; KGD, α-ketoglutarate decarboxylase; SSA DH, succinic semialdehyde dehydrogenase.

Inhibition of the respiratory electron transport chain shifts the redox state of the NADH/NAD^+ pool toward a more reduced state (43). Under these conditions, it could be possible that the glyoxylate shunt is favored to bypass the oxidative decarboxylation reactions of the TCA cycle between isocitrate and succinate to maintain NADH/ NAD^+ homeostasis, which might lead to an increase in carbon flux via the glyoxylate shunt, followed by induction of *icl1* expression.

Our RNA sequencing analysis (30) and reporter gene assay revealed that expression of *icl1* was derepressed in the Δ*crp1* mutant relative to that in the WT strain when the strains were grown on glucose (Fig. 8). This derepression did not occur during growth on acetate. Since we failed to obtain a Δ*crp1* Δ*crp2* double mutant of *M. smegmatis*, the involvement of Crp in the regulation of *icl1* expression was examined in the Δ*crp1* mutant, in which the *crp1* gene encoding the major Crp is inactivated. Due to the presence of Crp2 in the Δ*crp1* mutant, the extent of *icl1* repression by Crp in the WT strain of *M. smegmatis* grown on glucose might be greater than that extrapolated from the result in Fig. 8 using the Δ*crp1* mutant. The cellular level of cAMP in the WT strain grown on glucose or octanoate was shown to be approximately 2-fold higher than that in the WT grown on acetate (Fig. 9). Increased cAMP levels in glucose-grown cells are expected to enhance the functionality of Crp, leading to repression of *icl1* in glucose-grown *M. smegmatis*. Both a decrease in the cellular level of cAMP in acetate-grown cells relative to glucose-grown cells and the Crp (GlxR)-mediated negative regulation of the ICL gene have been previously reported for *C. glutamicum* (44, 45). Taken together, our findings suggest that the strong induction of *icl1* expression during growth on acetate as the sole carbon source relative to the weak expression of *icl1* in *M. smegmatis* grown on glucose is likely to result from combined effects of Crp-mediated repression of *icl1* in the presence of glucose and RamB-mediated induction of *icl1* in the presence of acetate. It is also conceivable that Crp might be to some extent responsible for the weak induction of *icl1* expression in *M. smegmatis* grown on octanoate relative to *M. smegmatis* grown on acetate.

It has been demonstrated in *C. glutamicum* that the LuxR-type transcriptional regulator RamA (Cg2831: regulator of acetate metabolism A) serves as an activator in the regulation of genes involved in acetate metabolism such as *aceA*, *pta*, and *ack* (46). *M. smegmatis* possesses a RamA homolog (MSMEG_5651) that shares 38% sequence identity and 57% similarity with RamA of *C. glutamicum*. We constructed a *ramA* deletion mutant of *M. smegmatis* and comparatively examined *icl1* expression in the WT and Δ*ramA* mutant strains. Inactivation of *ramA* did not result in changes in *icl1* expression in *M. smegmatis* grown on glucose or acetate, indicating that RamA is not involved in the regulation of *icl1* expression in *M. smegmatis* (Fig. S6).

Repression of *icl1* expression under particular conditions, such as inorganic phosphate (P_i)- or nitrogen-limiting conditions, has been recently reported for *M. smegmatis*. The *icl1* gene was demonstrated to be under the negative regulation of the P_i-sensing SenX3-RegX3 two-component system (47). We found that the suggested RegX3-binding operator is located immediately upstream of RamBS1, which implies that RegX3 bound at the operator might interfere with binding of RamB to RamBS1, leading to repression of *icl1* expression (Fig. S7). Analogously, GlnR, an orphan response regulator, was reported to negatively regulate *icl1* expression in *M. smegmatis* under nitrogen-limiting conditions. The reported GlnR-binding site overlaps RamBS2, indicating that GlnR represses *icl1* expression by occluding RamB binding to RamBS2 (41).

In conclusion, expression of the *icl1* gene encoding the major isocitrate lyase in *M. smegmatis* is regulated by RamB, which serves as the main regulator reflecting the cellular necessity of the glyoxylate shunt. Additionally, the cellular levels of cAMP as well as the availability of nitrogen sources and Pi are integrated by Crp1, GlnR, and the SenX3-RegX3 two-component system to exquisitely fine-tune expression of *icl1*.

MATERIALS AND METHODS

Bacterial strains, plasmids, and culture conditions. The bacterial strains and plasmids used in this study are listed in Table S1 in the supplemental material. *Escherichia coli* strains were grown in Luria-Bertani (LB) medium at 37°C. *M. smegmatis* strains were grown in Middlebrook 7H9 medium (Difco, Sparks, MD) supplemented with 0.2% (wt/vol) or 10 mM glucose, 10 mM acetate, or 2.5 mM octanoate as a carbon source and 0.02% (vol/vol) Tween 80 as an anticlumping agent at 37°C. *M. smegmatis* strains were grown aerobically in a 500-ml flask filled with 100 ml of growth medium on a gyratory shaker (200 rpm). Ampicillin (100 μg/ml for *E. coli*), chloramphenicol (34 μg/ml for *E. coli*), kanamycin (50 μg/ml for *E. coli* and 30 μg/ml for *M. smegmatis*), and hygromycin (200 μg/ml for *E. coli* and 50 or 25 μg/ml for *M. smegmatis*) were added to the growth medium when required. The construction of the mutants and the plasmids used in this study is described in the supplemental material.

DNA manipulation and electroporation. Standard protocols and manufacturers' instructions were followed for recombinant DNA manipulations (48). Transformation of *M. smegmatis* with plasmids was carried out by electroporation as described elsewhere (49). The primers used for PCR and site-directed mutagenesis are listed in Table S2.

***β*-Galactosidase assay.** The β-galactosidase activity was measured spectrophotometrically as described previously (50). The protein concentration was determined using a Bio-Rad protein assay kit (Bio-Rad, Hercules, CA) with bovine serum albumin (BSA) as a standard protein.

Protein purification. The *E. coli* BL21-Codonplus (DE3) strain harboring pET29bramB was grown aerobically at 37°C in LB medium containing 50 μg/ml of kanamycin and 34 μg/ml of chloramphenicol to an optical density at 600 nm (OD_{600}) of 0.6 to 0.7. Expression of the *ramB* genes was induced by the addition of isopropyl-β-D-thiogalactopyranoside (IPTG) to the cultures to a final concentration of 0.5 mM, and then cells were further grown for 6 h at 37°C. Cells were harvested from 500-ml cultures and resuspended in 10 ml of buffer A (20 mM Tris-HCl [pH 8.0], 200 mM NaCl, and 1 mM dithiothreitol [DTT]) containing DNase I (10 U/ml) and 10 mM $MgCl_2$. The resuspended cells were disrupted twice using a French pressure cell, and cell-free crude extracts were obtained by centrifugation twice at 20,000 $\times$ *g* for 15 min. The crude extracts were loaded into a column packed with 500 μl of the 80% (vol/vol) slurry of Ni-Sepharose high-performance resin (GE Healthcare, Piscataway, NJ). The resin was washed with 40 bed volumes of buffer A containing 5 mM imidazole and washed further with 40 bed volumes of buffer A containing 75 mM imidazole. His_6-tagged RamB was eluted from the resin with 6 bed volumes of buffer A containing 250 mM imidazole and 10% (vol/vol) glycerol. Imidazole and NaCl were removed from purified RamB by means of a PD-10 desalting column (GE Healthcare) equilibrated with 20 mM Tris-HCl (pH 8.0) containing 1 mM DTT and 10% (vol/vol) glycerol. His_6-tagged RamB was purified to near homogeneity (Fig. S8).

DNase I footprinting analysis. DNase I Footprinting was carried out using fluorescence (6-carboxytetramethylrhodamine [TAMRA])-labeled DNA fragments and purified RamB. A 369-bp TAMRA-labeled DNA fragment containing the *icl1* upstream region was generated by PCR using the F_TAMRA_pUC19 and R_icl1FootF primers. The pUC19icl1FootF and pUC19icl1FootR plasmids were used for PCR as templates to generate DNA fragments with the TAMRA-labeled coding and noncoding strands, respectively. The PCR products were purified after agarose gel electrophoresis, and the DNA concentration was determined using a Multiskan SkyHigh microplate spectrophotometer (Thermo Fisher, Waltham, MA). DNA binding reaction mixtures were composed of 5 pmol of labeled DNA probes, various amounts of purified RamB, 20 mM Tris-HCl (pH 8.0), 0.2 mM $MgCl_2$, 2.1 mM KCl, 0.04 mM DTT, and 11.1% (vol/vol) glycerol in a final volume of 190 μl. When necessary, the RamB protein was treated with 200 μM succinyl-CoA. The mixture was incubated for 10 min at 25°C prior to DNase I treatment. DNase I treatment, DNA purification, and electrophoresis on 6% (wt/vol) denaturing polyacrylamide gels were performed as described previously (30). Reference sequencing was performed by using a Thermo Sequenase dye primer manual cycle sequencing kit (Thermo Fisher) with the primer F_TAMRA_pUC19 and the template plasmid (pUC19icl1FootF or pUC19icl1FootR).

EMSA. A 184-bp DNA fragment containing the upstream region of *icl1* and a 145-bp control DNA fragment without the RamB-binding site were used in EMSA. The 184-bp DNA fragment was amplified by PCR using pUC19icl1FootF as a template and the F_icl1EMSA and R_icl1EMSA primers. The 145-bp control DNA fragment was generated by PCR using pUC19 as a template and the F_EMSAns and R_EMSAns primers. Purified RamB protein was incubated with 90 fmol of the DNA fragments containing the *icl1* upstream region and 90 fmol of the control DNA fragments in binding buffer (20 mM Tris-HCl [pH 8.0], 2.5 mM $MgCl_2$, and 1 mM DTT) in a reaction volume of 10 μl for 20 min at 25°C. To examine the effect of succinyl-CoA, succinate, acetate, and acetyl phosphate on the binding of RamB to the DNA fragments, 200 μM succinyl-CoA, succinate, acetate, and acetyl phosphate were included in the DNA-protein mixtures. After the addition of 2 μl of 6$\times$ loading buffer (0.25% [wt/vol] bromophenol blue, 0.25% [wt/vol] xylene cyanol, and 40% [wt/vol] sucrose), the mixtures were subjected to nondenaturing PAGE (6% [wt/vol] acrylamide) using 0.5$\times$ TBE buffer (41.5 mM Tris-borate [pH 8.3] and 0.5 mM EDTA) at 70 V for 1 h 45 min at 4°C. The gels were stained with SYBR green staining solution (Invitrogen, Waltham, MA) for 1 h.

Determination of the intracellular cAMP concentration. *M. smegmatis* cells corresponding to 1 ml of cultures at an OD_{600} of 0.4 were harvested. Cell pellets were resuspended in 1 ml of sample diluent concentrate buffer (Arbor Assays, Ann Arbor, MI) and then incubated for 10 min. Cells were disrupted once by using a Fastprep 120 bead beater (Thermo Fisher, Waltham, MA) at 5.0 m/s for 45 s. Cell-free supernatants were obtained by centrifugation at 20,000 $\times$ *g* for 10 min. The concentration of cAMP in the prepared supernatants was determined by using a DetectX cyclic AMP direct immunoassay kit (Arbor Assays) and a microplate reader (Thermo Fisher) following the manufacturers' instructions.

NMR analysis. *M. smegmatis* cells were grown aerobically to an OD_{600} of 0.5 in 7H9 medium supplemented with 10 mM glucose or 10 mM acetate. Fifty milliliters of culture was harvested by centrifugation at 5,000 $\times$ *g* for 5 min at 4°C. Extraction of intracellular metabolites was performed as described previously (51). Briefly, the cell pellets were resuspended in 1 ml of 95% acetonitrile and 25 mM formic acid and disrupted by vigorous vortexing 10 times for 1 min. Samples were chilled on ice between vortexings for 5 min. Cell-free extracts were obtained following centrifugation at 15,000 $\times$ *g* for 10 min at 4°C. The obtained extracts were mixed with 10 ml of deionized water. To retrieve the residual metabolites from the cell pellet, the cell pellets were washed with 8 ml of deionized water once. After centrifugation at 15,000 $\times$ *g* for 10 min at 4°C, the obtained supernatants were mixed with the extracts and subjected to lyophilization. The lyophilized samples were redissolved using 500 μl of resuspension buffer (25 mM ammonium formate [pH 3.0], 2% methanol). For nuclear magnetic resonance (NMR) measurement, 20-μl volumes of redissolved samples were placed in a 4-mm NMR nanotube (Agilent; 4-mm sample tube) with 20 μl of phosphate buffer (pH 7.4 in deuterated water) containing 4 mM sodium 3-trimethylshily-2,2,3,3-d4 -propionate (TSP-d_4) as a reference of chemical shift (0.00 ppm) and quantification. ^{1}H NMR spectra were obtained using a 600-MHz high-resolution magic-angle spinning (HR-MAS) NMR spectrometer with a nano-NMR probe (Agilent Technologies, Santa Clara, CA) at a degree of magic angle of 54.74° and a spinning rate of 2,000 Hz. For NMR data of each sample, the Carr-Purcell-Meiboom-Gill (CPMG) pulse was applied, and spectra were acquired using a 3-s relaxation delay time and 3-s acquisition time at a temperature of 298 K. A total of 128 scans were collected, and total acquisition time was 13 min 9 s. All spectra were processed and assigned using Chenomx NMR Suite 8.4 professional with the Chenomx 600-MHz library database (Chenomx Inc., Edmonton, Canada).

SUPPLEMENTAL MATERIAL

Supplemental material is available online only.
SUPPLEMENTAL FILE 1, PDF file, 1.3 MB.

ACKNOWLEDGMENT

This research was supported by the Basic Science Research Program through the National Research Foundation of Korea (NRF) funded by the Ministry of Education, Science and Technology (NRF-2020R1A2C1005305).

REFERENCES

1. Dolan SK, Welch M. 2018. The glyoxylate shunt, 60 years on. Annu Rev Microbiol 72:309–330. https://doi.org/10.1146/annurev-micro-090817-062257.
2. McKinney JD, Honer zu Bentrup K, Munoz-Elias EJ, Miczak A, Chen B, Chan WT, Swenson D, Sacchettini JC, Jacobs WR, Jr, Russell DG. 2000. Persistence of *Mycobacterium tuberculosis* in macrophages and mice requires

the glyoxylate shunt enzyme isocitrate lyase. Nature 406:735–738. https://doi.org/10.1038/35021074.

3. Munoz-Elias EJ, McKinney JD. 2005. *Mycobacterium tuberculosis* isocitrate lyases 1 and 2 are jointly required for in vivo growth and virulence. Nat Med 11:638–644. https://doi.org/10.1038/nm1252.
4. Munoz-Elias EJ, McKinney JD. 2006. Carbon metabolism of intracellular bacteria. Cell Microbiol 8:10–22. https://doi.org/10.1111/j.1462-5822.2005.00648.x.
5. Munoz-Elias EJ, Upton AM, Cherian J, McKinney JD. 2006. Role of the methylcitrate cycle in *Mycobacterium tuberculosis* metabolism, intracellular growth, and virulence. Mol Microbiol 60:1109–1122. https://doi.org/10.1111/j.1365-2958.2006.05155.x.
6. Russell DG, Cardona PJ, Kim MJ, Allain S, Altare F. 2009. Foamy macrophages and the progression of the human tuberculosis granuloma. Nat Immunol 10:943–948. https://doi.org/10.1038/ni.1781.
7. Upton AM, McKinney JD. 2007. Role of the methylcitrate cycle in propionate metabolism and detoxification in *Mycobacterium smegmatis*. Microbiology (Reading) 153:3973–3982. https://doi.org/10.1099/mic.0.2007/011726-0.
8. Gould TA, van de Langemheen H, Munoz-Elias EJ, McKinney JD, Sacchettini JC. 2006. Dual role of isocitrate lyase 1 in the glyoxylate and methylcitrate cycles in *Mycobacterium tuberculosis*. Mol Microbiol 61:940–947. https://doi.org/10.1111/j.1365-2958.2006.05297.x.
9. Eoh H, Rhee KY. 2014. Methylcitrate cycle defines the bactericidal essentiality of isocitrate lyase for survival of *Mycobacterium tuberculosis* on fatty acids. Proc Natl Acad Sci U S A 111:4976–4981. https://doi.org/10.1073/pnas.1400390111.
10. Bhusal RP, Jiao W, Kwai BXC, Reynisson J, Collins AJ, Sperry J, Bashiri G, Leung IKH. 2019. Acetyl-CoA-mediated activation of *Mycobacterium tuberculosis* isocitrate lyase 2. Nat Commun 10:4639. https://doi.org/10.1038/s41467-019-12614-7.
11. Chopra T, Hamelin R, Armand F, Chiappe D, Moniatte M, McKinney JD. 2014. Quantitative mass spectrometry reveals plasticity of metabolic networks in *Mycobacterium smegmatis*. Mol Cell Proteomics 13:3014–3028. https://doi.org/10.1074/mcp.M113.034082.
12. Honer Zu Bentrup K, Miczak A, Swenson DL, Russell DG. 1999. Characterization of activity and expression of isocitrate lyase in *Mycobacterium avium* and *Mycobacterium tuberculosis*. J Bacteriol 181:7161–7167. https://doi.org/10.1128/JB.181.23.7161-7167.1999.
13. Micklinghoff JC, Breitinger KJ, Schmidt M, Geffers R, Eikmanns BJ, Bange FC. 2009. Role of the transcriptional regulator RamB (Rv0465c) in the control of the glyoxylate cycle in *Mycobacterium tuberculosis*. J Bacteriol 191:7260–7269. https://doi.org/10.1128/JB.01009-09.
14. Graham JE, Clark-Curtiss JE. 1999. Identification of *Mycobacterium tuberculosis* RNAs synthesized in response to phagocytosis by human macrophages by selective capture of transcribed sequences (SCOTS). Proc Natl Acad Sci U S A 96:11554–11559. https://doi.org/10.1073/pnas.96.20.11554.
15. Muttucumaru DG, Roberts G, Hinds J, Stabler RA, Parish T. 2004. Gene expression profile of *Mycobacterium tuberculosis* in a non-replicating state. Tuberculosis (Edinb) 84:239–246. https://doi.org/10.1016/j.tube.2003.12.006.
16. Saxena A, Srivastava V, Srivastava R, Srivastava BS. 2008. Identification of genes of *Mycobacterium tuberculosis* upregulated during anaerobic persistence by fluorescence and kanamycin resistance selection. Tuberculosis (Edinb) 88:518–525. https://doi.org/10.1016/j.tube.2008.01.003.
17. Tang YJ, Shui W, Myers S, Feng X, Bertozzi C, Keasling JD. 2009. Central metabolism in *Mycobacterium smegmatis* during the transition from O_2-rich to O_2-poor conditions as studied by isotopomer-assisted metabolite analysis. Biotechnol Lett 31:1233–1240. https://doi.org/10.1007/s10529-009-9991-7.
18. Stackebrandt E, Rainey FA, Ward-Rainey NL. 1997. Proposal for a new hierarchic classification system, *Actinobacteria* classis nov. Int J Syst Evol Microbiol 47:479–491. https://doi.org/10.1099/00207713-47-2-479.
19. Gerstmeir R, Cramer A, Dangel P, Schaffer S, Eikmanns BJ. 2004. RamB, a novel transcriptional regulator of genes involved in acetate metabolism of *Corynebacterium glutamicum*. J Bacteriol 186:2798–2809. https://doi.org/10.1128/JB.186.9.2798-2809.2004.
20. Auchter M, Cramer A, Huser A, Ruckert C, Emer D, Schwarz P, Arndt A, Lange C, Kalinowski J, Wendisch VF, Eikmanns BJ. 2011. RamA and RamB are global transcriptional regulators in *Corynebacterium glutamicum* and control genes for enzymes of the central metabolism. J Biotechnol 154:126–139. https://doi.org/10.1016/j.jbiotec.2010.07.001.
21. Xie L, Wang X, Zeng J, Zhou M, Duan X, Li Q, Zhang Z, Luo H, Pang L, Li W, Liao G, Yu X, Li Y, Huang H, Xie J. 2015. Proteome-wide lysine acetylation profiling of the human pathogen *Mycobacterium tuberculosis*. Int J Biochem Cell Biol 59:193–202. https://doi.org/10.1016/j.biocel.2014.11.010.
22. Zhou M, Xie L, Yang Z, Zhou J, Xie J. 2017. Lysine succinylation of *Mycobacterium tuberculosis* isocitrate lyase (ICL) fine-tunes the microbial resistance to antibiotics. J Biomol Struct Dyn 35:1030–1041. https://doi.org/10.1080/07391102.2016.1169219.
23. Bi J, Wang Y, Yu H, Qian X, Wang H, Liu J, Zhang X. 2017. Modulation of central carbon metabolism by acetylation of isocitrate lyase in *Mycobacterium tuberculosis*. Sci Rep 7:44826. https://doi.org/10.1038/srep44826.
24. Nandakumar M, Nathan C, Rhee KY. 2014. Isocitrate lyase mediates broad antibiotic tolerance in *Mycobacterium tuberculosis*. Nat Commun 5:4306. https://doi.org/10.1038/ncomms5306.
25. Lee HN, Ji CJ, Lee HH, Park J, Seo YS, Lee JW, Oh JI. 2018. Roles of three FurA paralogs in the regulation of genes pertaining to peroxide defense in *Mycobacterium smegmatis* mc^2 155. Mol Microbiol 108:661–682. https://doi.org/10.1111/mmi.13956.
26. Masiewicz P, Brzostek A, Wolański M, Dziadek J, Zakrzewska-Czerwińska J. 2012. A novel role of the PrpR as a transcription factor involved in the regulation of methylcitrate pathway in *Mycobacterium tuberculosis*. PLoS One 7:e43651. https://doi.org/10.1371/journal.pone.0043651.
27. Tang S, Hicks ND, Cheng YS, Silva A, Fortune SM, Sacchettini JC. 2019. Structural and functional insight into the *Mycobacterium tuberculosis* protein PrpR reveals a novel type of transcription factor. Nucleic Acids Res 47:9934–9949. https://doi.org/10.1093/nar/gkz724.
28. Sharma R, Zaveri A, Gopalakrishnapai J, Srinath T, Thiruneelakantan S, Varshney U, Visweswariah SS. 2014. Paralogous cAMP receptor proteins in *Mycobacterium smegmatis* show biochemical and functional divergence. Biochemistry 53:7765–7776. https://doi.org/10.1021/bi500924v.
29. Aung HL, Dixon LL, Smith LJ, Sweeney NP, Robson JR, Berney M, Buxton RS, Green J, Cook GM. 2015. Novel regulatory roles of cAMP receptor proteins in fast-growing environmental mycobacteria. Microbiology (Reading) 161:648–661. https://doi.org/10.1099/mic.0.000015.
30. Ko EM, Oh JI. 2020. Induction of the *cydAB* operon encoding the *bd* quinol oxidase under respiration-inhibitory conditions by the major cAMP receptor protein MSMEG_6189 in *Mycobacterium smegmatis*. Front Microbiol 11:608624. https://doi.org/10.3389/fmicb.2020.608624.
31. Murima P, Zimmermann M, Chopra T, Pojer F, Fonti G, Dal Peraro M, Alonso S, Sauer U, Pethe K, McKinney JD. 2016. A rheostat mechanism governs the bifurcation of carbon flux in mycobacteria. Nat Commun 7:12527. https://doi.org/10.1038/ncomms12527.
32. Raibaud O, Schwartz M. 1984. Positive control of transcription initiation in bacteria. Annu Rev Genet 18:173–206. https://doi.org/10.1146/annurev.ge.18.120184.001133.
33. Collado-Vides J, Magasanik B, Gralla JD. 1991. Control site location and transcriptional regulation in *Escherichia coli*. Microbiol Rev 55:371–394. https://doi.org/10.1128/mr.55.3.371-394.1991.
34. Wagner T, Bellinzoni M, Wehenkel A, O'Hare HM, Alzari PM. 2011. Functional plasticity and allosteric regulation of alpha-ketoglutarate decarboxylase in central mycobacterial metabolism. Chem Biol 18:1011–1020. https://doi.org/10.1016/j.chembiol.2011.06.004.
35. Baughn AD, Garforth SJ, Vilcheze C, Jacobs WR, Jr. 2009. An anaerobic-type alpha-ketoglutarate ferredoxin oxidoreductase completes the oxidative tricarboxylic acid cycle of *Mycobacterium tuberculosis*. PLoS Pathog 5:e1000662. https://doi.org/10.1371/journal.ppat.1000662.
36. Tian J, Bryk R, Shi S, Erdjument-Bromage H, Tempst P, Nathan C. 2005. *Mycobacterium tuberculosis* appears to lack alpha-ketoglutarate dehydrogenase and encodes pyruvate dehydrogenase in widely separated genes. Mol Microbiol 57:859–868. https://doi.org/10.1111/j.1365-2958.2005.04741.x.
37. Tian J, Bryk R, Itoh M, Suematsu M, Nathan C. 2005. Variant tricarboxylic acid cycle in *Mycobacterium tuberculosis*: identification of alpha-ketoglutarate decarboxylase. Proc Natl Acad Sci U S A 102:10670–10675. https://doi.org/10.1073/pnas.0501605102.
38. de Carvalho LP, Fischer SM, Marrero J, Nathan C, Ehrt S, Rhee KY. 2010. Metabolomics of *Mycobacterium tuberculosis* reveals compartmentalized co-catabolism of carbon substrates. Chem Biol 17:1122–1131. https://doi.org/10.1016/j.chembiol.2010.08.009.
39. O'Hare HM, Duran R, Cervenansky C, Bellinzoni M, Wehenkel AM, Pritsch O, Obal G, Baumgartner J, Vialaret J, Johnsson K, Alzari PM. 2008. Regulation of glutamate metabolism by protein kinases in mycobacteria. Mol Microbiol 70:1408–1423. https://doi.org/10.1111/j.1365-2958.2008.06489.x.
40. Beste DJ, Bonde B, Hawkins N, Ward JL, Beale MH, Noack S, Noh K, Kruger NJ, Ratcliffe RG, McFadden J. 2011. ^{13}C metabolic flux analysis identifies an unusual route for pyruvate dissimilation in mycobacteria which

requires isocitrate lyase and carbon dioxide fixation. PLoS Pathog 7: e1002091. https://doi.org/10.1371/journal.ppat.1002091.

41. Qi N, She GL, Du W, Ye BC. 2021. *Mycobacterium smegmatis* GlnR regulates the glyoxylate cycle and the methylcitrate cycle on fatty acid metabolism by repressing *icl* transcription. Front Microbiol 12:603835. https://doi.org/10.3389/fmicb.2021.603835.
42. Jakoby WB, Scott EM. 1959. Aldehyde oxidation. III. Succinic semialdehyde dehydrogenase. J Biol Chem 234:937–940. https://doi.org/10.1016/S0021-9258(18)70207-X.
43. Jeong JA, Park SW, Yoon D, Kim S, Kang HY, Oh JI. 2018. Roles of alanine dehydrogenase and induction of its gene in *Mycobacterium smegmatis* under respiration-inhibitory conditions. J Bacteriol 200:e00152-18. https://doi.org/10.1128/JB.00152-18.
44. Kim HJ, Kim TH, Kim Y, Lee HS. 2004. Identification and characterization of *glxR*, a gene involved in regulation of glyoxylate bypass in *Corynebacterium glutamicum*. J Bacteriol 186:3453–3460. https://doi.org/10.1128/JB.186.11.3453-3460.2004.
45. Park SY, Moon MW, Subhadra B, Lee JK. 2010. Functional characterization of the *glxR* deletion mutant of *Corynebacterium glutamicum* ATCC 13032: involvement of GlxR in acetate metabolism and carbon catabolite repression. FEMS Microbiol Lett 304:107–115. https://doi.org/10.1111/j.1574-6968.2009.01884.x.
46. Cramer A, Gerstmeir R, Schaffer S, Bott M, Eikmanns BJ. 2006. Identification of RamA, a novel LuxR-type transcriptional regulator of genes involved in acetate metabolism of *Corynebacterium glutamicum*. J Bacteriol 188:2554–2567. https://doi.org/10.1128/JB.188.7.2554-2567.2006.
47. Pei JF, Qi N, Li YX, Wo J, Ye BC. 2021. RegX3-mediated regulation of methylcitrate cycle in *Mycobacterium smegmatis*. Front Microbiol 12:619387. https://doi.org/10.3389/fmicb.2021.619387.
48. Sambrook J, Green MR. 2012. Molecular cloning: a laboratory manual, 4th ed. Cold Spring Harbor Laboratory Press, Cold Spring Harbor, NY.
49. Snapper SB, Melton RE, Mustafa S, Kieser T, Jacobs WR, Jr. 1990. Isolation and characterization of efficient plasmid transformation mutants of *Mycobacterium smegmatis*. Mol Microbiol 4:1911–1919. https://doi.org/10.1111/j.1365-2958.1990.tb02040.x.
50. Oh JI, Kaplan S. 1999. The *cbb3* terminal oxidase of *Rhodobacter sphaeroides* 2.4.1: structural and functional implications for the regulation of spectral complex formation. Biochemistry 38:2688–2696. https://doi.org/10.1021/bi9825100.
51. Glaser L, Kuhl M, Jovanovic S, Fritz M, Vogeli B, Erb TJ, Becker J, Wittmann C. 2020. A common approach for absolute quantification of short chain CoA thioesters in prokaryotic and eukaryotic microbes. Microb Cell Fact 19:160. https://doi.org/10.1186/s12934-020-01413-1.